Characterization of corneal structure in keratoconus

David P. Piñero, PhD, Juan C. Nieto, MSc, Alberto Lopez-Miguel, MSc

The increasing volume of patients interested in refractive surgery and the new treatment options available for keratoconus have generated a higher interest in achieving a better characterization of this pathology. The ophthalmic devices for corneal analysis and diagnosis have experienced a rapid development during the past decade with the implementation of technologies such as the Placido-disk corneal topography and the introduction of others such as scanning-slit topography, Scheimpflug photography, and optical coherence tomography, which are able to accurately describe not only the geometry of the anterior corneal surface but also that of the posterior surface, as well as pachymetry and corneal volume. Specifically, anterior and posterior corneal elevation, corneal power, pachymetry maps, and corneal coma-like aberrometry data provide sufficient information for an accurate characterization of the cornea to avoid misleading diagnoses of patients and provide appropriate counseling of refractive surgery candidates.

Financial Disclosure: No author has a financial or proprietary interest in any material or method mentioned.

J Cataract Refract Surg 2012; 38:2167–2183 © 2012 ASCRS and ESCRS

Keratoconus is an ectatic corneal disorder characterized by a usually progressive corneal thinning that results in corneal protrusion, irregular astigmatism, and decreased vision.[1] Specifically, the cornea assumes a conical shape as a result of the degeneration of the corneal stromal tissue and the subsequent biomechanical alteration.[1,2] The incidence of this condition varies depending on factors such as the ethnic group analyzed or the criteria used to establish the diagnosis; most estimates are between 50 and 230 per 100 000 in the general population.[1] Several risk factors, such as constant eye rubbing, the presence of systemic diseases (eg, sleep apnea), floppy eyelid syndrome, allergies, and eczema, as well as family history, have been defined for the development of this corneal disease.[1]

Corneal topography is a valuable tool for confirming the keratoconus diagnosis.[1] Several indices, algorithms, and even neural network approaches to the geometry and optical properties of the anterior corneal surface have been developed for keratoconus diagnosis and detection.[3–13] Therefore, moderate and advanced keratoconus detection is not a difficult issue using corneal topography in combination with biomicroscopic, retinoscopic, and pachymetric evaluation.[1] Detection problems arise with very early or preclinical stages of the ectatic disorder. The term *keratoconus suspect* was coined for designating corneas not showing biomicroscopic keratoconic signs but subtle topographic features similar to early stages of keratoconus.[14–19] In such conditions, other diagnostic tests and examinations may be helpful to confirm the potential presence of an incipient ectatic condition.

The biomicroscopic findings in keratoconus, such as stromal thinning and posterior stress line, suggest that posterior corneal geometry may be altered independently of the anterior surface alterations. There is evidence that both anterior and posterior curvatures are affected in keratoconic eyes and also in keratoconus suspect eyes.[20] Likewise, significantly larger values of best-fit sphere (BFS)[14,16,21] and posterior

Submitted: October 23, 2011.
Final revision submitted: February 8, 2012.
Accepted: May 28, 2012.

From the Department of Ophthalmology, Oftalmar (Piñero), Hospital Internacional Medimar, the Foundation for the Visual Quality (Piñero), Fundación para la Calidad Visual, the Optics, Pharmacology and Anatomy Department (Piñero), University of Alicante, Alicante, the Optometry and Vision Sciences Unit (Nieto), Optics Department, University of Valencia, the Avanza Vision Ophthalmology Clinic (Nieto), Valencia, and the Institute of Applied Ophthalmobiology (Lopez-Miguel), University of Valladolid, Valladolid, Spain.

Corresponding author: David P. Piñero, PhD, Oftalmar, Department of Ophthalmology, Medimar International Hospital, Avenida Denia, 78, 03016 Alicante, Spain. E-mail: david.pinyero@ua.es.

© 2012 ASCRS and ESCRS
Published by Elsevier Inc.

http://dx.doi.org/10.1016/j.jcrs.2012.10.022

elevation[15,16,22] have been reported in clinical keratoconic eyes and keratoconus suspect eyes. Therefore, manifestations of the ectasia also occur at the posterior corneal surface, even in early stages of the disease. These manifestations can be currently monitored in the clinical practice by means of advanced imaging techniques that are commercially available, such as optical coherence tomographers, systems combining the scanning-slit and Placido disk technologies, and systems based on Scheimpflug photography.[23] These systems also allow the clinician to characterize the pachymetric distribution as well as the volume of the evaluated cornea, which have been shown to be useful for keratoconus diagnosis and characterization.[24]

The aim of the current review is to summarize the diagnostic criteria defined for keratoconus with the more advanced topography systems, including analysis of the posterior corneal surface and pachymetric distribution. These criteria are especially useful for screening corneal refractive surgery candidates to avoid performing the surgical procedure in a pathological or potentially pathological cornea.

ANALYSIS OF THE ANTERIOR CORNEAL SURFACE IN KERATOCONUS

Analysis of the Topographic Map

Analysis of the topographic pattern of the anterior corneal surface has been shown to help identify ectatic corneas, especially during the early states because the topographic pattern in such conditions is different than the normal pattern.[1,25–28] Many studies have been conducted to characterize the keratoconus "topographical phenotype" by means of computerized corneal videokeratography.[1,12,29,30] In most patients affected by keratoconus, the topographic map of the anterior corneal surface is characterized by focal steepening over the peripheral or midperipheral zone, which coincides with the location of the conical protrusion that commonly expands over fewer than 2 quadrants.[1] Therefore, the typical appearance of the keratoconic topographic map is the presence of a well-delimited zone with a high dioptric value, surrounded by progressively decreasing curvature zones (Figure 1). The cone vertex is typically displaced toward the lower midperipheral region in either the nasal or temporal quadrant, although in rare occasions the ectatic alterations could appear in the central portion of the cornea. In contrast to a with-the-rule topographical astigmatism in a healthy cornea, the topographical keratoconic loop is usually asymmetric with an inferior hemimeridian showing steeper radii (Figure 1). Likewise, there is usually a vertical asymmetry with a certain diagonal angling for any of the 2 hemimeridians, providing a characteristic topographic image pattern. This topographic pattern is commonly similar in both eyes, although one of them may show a more advanced state.

As a summary, the topographic pattern of keratoconus usually has several particular features (Figure 1): (1) Focal steepening located in the cone protrusion zone surrounded by concentric decreasing power zones. Focal areas with dioptric values greater than 46.0 to 47.0 diopters (D) should alert the examiner and other diagnostic complementary tests must be performed to confirm or rule out the

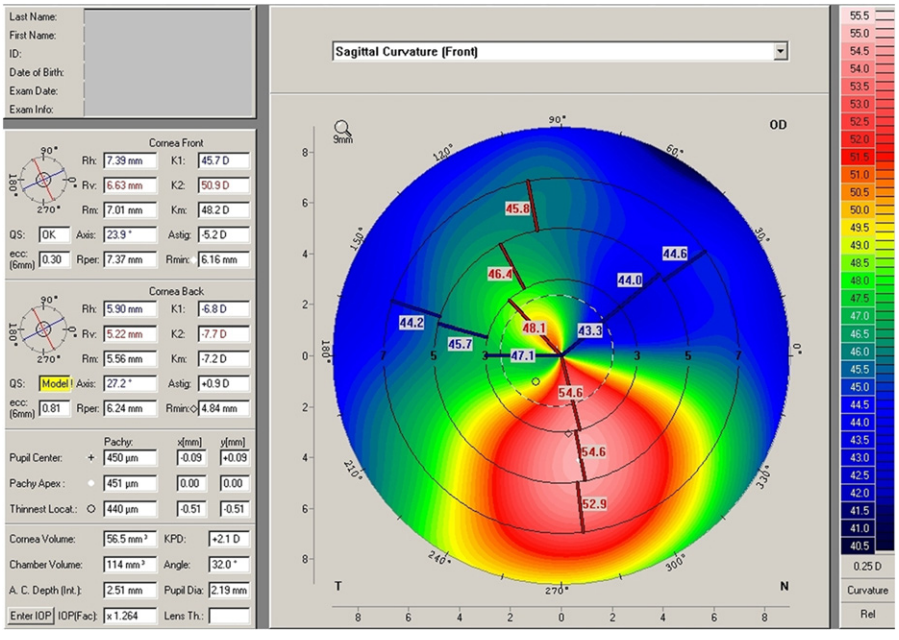

Figure 1. Axial curvature map of a keratoconic cornea obtained by a rotating Scheimpflug camera device.

diagnosis of keratoconus. (2) Inferior–superior (I–S) asymmetry within the midperipheral cornea. Special attention should be taken when obtaining values of the I–S index greater than 1.4 D. (3) Angling of the hemimeridians in the bowtie pattern. Keratoconus must be suspected, especially when this angling exceeds 20 or 30 degrees in relation to the vertical meridian.

Several topographic maps of the anterior corneal surface can be useful in detecting and characterizing the keratoconus, such as the tangential or elevation maps. As tangential maps provide more detailed information about local changes in curvature than axial maps,[31] the tangential algorithm has been shown to be more valid for the clinical identification of topographical patterns compatible with keratoconus.[32–37] Tangential maps combined with elevation (front and posterior) and pachymetric maps are an excellent tool for keratoconus detection, even in the most incipient forms.

The color scale used to graphically show the topographic data must be selected with care. Several studies of the ideal dioptric step for topographical scaling have been published, with the aim of defining a standard for obtaining the maximum information from the diagnostic examination.[38–40] The American National Standards Institute[39] suggest the use of 0.5, 1.0, and 1.5 D steps as adequate intervals. Smolek et al.[38] report that the standard deviation (SD) for curvature in the central corneal portion of a normal group of corneas was 1.59 D, stating that the use of 1.5 D steps was optimum for color topographic scaling. Similarly, in their clinical study using a standard videokeratograph, Wilson et al.[40] conclude that no topographical discoveries were unnoticed using a 1.5 D step instead of 1.0 D.

Corneal Asphericity

Some quantitative indexes and descriptors have been defined or developed for characterizing the shape of the anterior corneal surface (Table 1). One of the most important is the corneal asphericity. It should be considered that the geometry of the anterior corneal surface of the human cornea can be adjusted to a conical section that is characterized by an asphericity (Q) and a specific value for the radius of the apical curvature (r_0).[41,42] The Q characterizes the gradual curvature change in the corneal surface from center to periphery.[42–44] The most commonly accepted value for Q in young adult patients is -0.23 ± 0.08 (prolate ellipsoid).[41,45] Positive values of Q would denote the presence of an oblate surface (ie, corneas after myopic ablation with the excimer laser or orthokeratology treatments), and a null value ($Q = 0$) would represent a completely spherical surface. In an ectatic cornea (Figure 2), the anterior protrusion generates an increase of the corneal prolatism with an associated negativization of Q (Table 1). Indeed, a more marked negative asphericity (significant prolateness) for the anterior corneal surface was reported in a study by Piñero et al.[46] comparing some topographic features of a sample of normal eyes with those found in keratoconic corneas grade I and II according to the Amsler-Krumeich grading system.[4] Specifically, mean Q values of -0.29 ± 0.09, -0.65 ± 0.27, and -1.18 ± 0.32 were found in the normal, keratoconus grade I, and keratoconus grade II groups, respectively.[46] It should be mentioned that other related parameters are used by some authors for representing the corneal curvature change from center to periphery: eccentricity (e), $Q = -e^2$; form factor (p), $p = 1 + Q$; shape factor, shape factor $= -Q$.

Table 1. Values of asphericity and the related parameters for the conic surfaces that may adjust to the anterior corneal contour.

Curve	e^2	p	Q
Hyperbola	>1	<0	<-1
Parabola	1	0	-1
Prolate ellipsoid	$0 < e^2 < 1$	$0 < p < 1$	$-1 < Q < 0$
Sphere	0	1	0
Oblate ellipsoid	< 0	> 1	> 0

e^2 = eccentricity; p = shape factor; Q = asphericity

Other Indexes and Descriptors

Several topographic indexes and descriptors have been developed for characterizing corneal shape that can be especially useful for the detection and diagnosis of keratoconus. Some of the most common indices are the corneal irregularity measurement (CIM), the mean toric keratometry (MTK), the surface regularity index (SRI), the predicted corneal acuity (PCA), and the surface asymmetry index (SAI). The CIM is a numeric value representing the degree of irregularity that is present in the corneal surface and obtained by means of a proprietary algorithm.[47] Higher probability of a pathological cornea is associated with large values of this index. The CIM is graded with the following criteria[47]: healthy from 0.03 to 0.68 μm, borderline from 0.69 to 1.00 μm, and anomalous from 1.10 to 5.00 μm. The MTK is derived from corneal elevation data. It compares the analyzed cornea with the elevation values obtained by means of the best-fit toric surface.[47] The larger the MTK value, the more significant is the corneal toricity and the higher is the likelihood of a corneal ectatic disorder. The MTK distribution in the

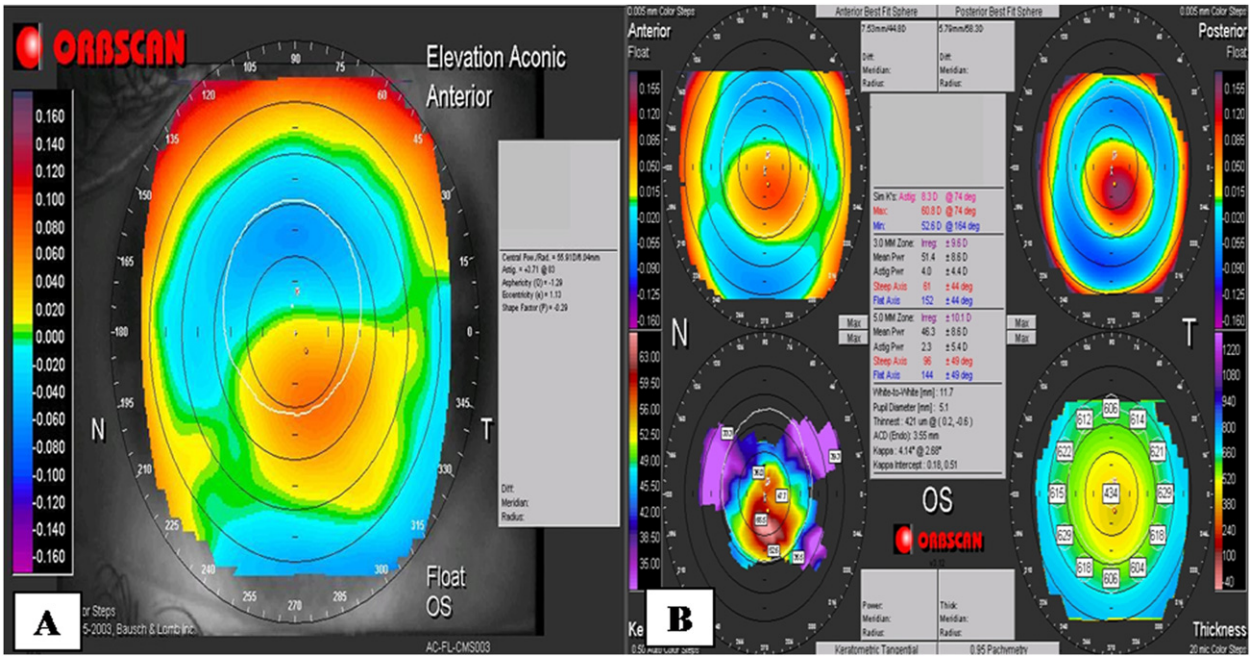

Figure 2. *A*: Front elevation map of a keratoconus. The descriptive parameters (Q = −1.29, e = 1.13) show high prolate values. These values are a result of the cone protrusion. *B*: High progressive keratoconus showing localized paracentral protrusion, pachymetry thinning, and high posterior steepening.

population resembles the Gaussian bell curve, with an average value of 44.5 D and values for this index ranging from 41.25 to 47.25 D for 96% of the population. The MTK is graded with the following criteria[47]: healthy from 43.1 to 45.9 D, borderline from 41.8 to 43.0 D and from 46.0 to 47.2 D, and anomalous from 36.0 to 41.7 and from 47.3 to 60.0 D.

The SRI, described by Wilson and Klyce in 1991,[48] is a corneal quantitative descriptor. It attempts to represent localized fluctuations in the corneal surface along a meridian within the central corneal area. This descriptor has been shown to be highly correlated with the corrected visual acuity ($\rho = 0.80$, $P < .001$). A cornea considered as normal and healthy presents values of SRI below 1.55.

The PCA is a quantitative index that provides information about the corneal optical quality within the 3.0 mm central area.[9] It is one of the 15 corneal parameters provided by the Holladay diagnosis system in Eyesys videokeratographs (EyeSys Vision).[9] Finally, the SAI is a centrally weighted summation of differences in corneal power between corresponding points 180 degrees apart on 128 equally spaced meridians.[13] This index approaches zero for a radially symmetrical surface and increases as the corneal shape becomes more asymmetrical.[13]

Screening Systems

With the aim of providing faster and better classification of topographic patterns of the anterior corneal surface, several diagnostic or early detection software and algorithms have been developed and incorporated into corneal topography systems.[9,48–52] The most commonly used are described below.

The Pathfinder Corneal Analysis module, which is included in the Atlas videokeratograph (anterior corneal topography analyzer) software (Carl Zeiss Meditec AG), allows the detection of irregular topographic conditions compatible with keratoconus.[47,49] It is based on the combined analysis of the quantitative descriptors CIM, shape factor, and MTK. The algorithm used classifies the result of the analysis as follows:

Normal: The cornea shows a typically aspheric profile with CIM, shape factor, and MTK values within normal limits.

Corneal distortion, also called pseudokeratoconus: This is corneal molding or warpage usually derived from contact lens wear. It is characterized by a CIM value outside the normal range but with normal shape factor and MTK values.

Subclinical keratoconus (keratoconus suspect by definition): The topographic pattern usually shows an I–S asymmetry with curvature values lower than 50.0 D at the cone apex. The CIM and MTK values are usually outside the normal range, whereas the shape factor is normal or slightly outside normality.

Keratoconus: The topographic map alteration is evident, with CIM, MTK, and shape factor outside normal limits.

Another keratoconus screening algorithm is described by Rabinowitz[51] and based on the use of 2 descriptive parameters: the central keratometry (K) value and the I–S index. The I–S index characterizes the dioptric asymmetry between the superior and inferior corneal hemispheres. According to these detection criteria, the cornea can be classified as normal, keratoconus suspect, or clinical keratoconus. Specifically, the cornea is considered as keratoconus suspect when either the central K value or the I–S index value is above the magnitude obtained by adding 2 times the SD to the mean value; it is considered as keratoconus when at least 1 of the 2 indexes is above 3 times the SD added to the mean value.[51] The modified Rabinowitz-McDonnell criteria[12] were derived from these initial detection criteria, using the same descriptive parameters, central K value and I–S index. These criteria established that a cornea is susceptible to be catalogued as keratoconus when the central K value is equal to or above 47.2 D, the value of the I–S index is equal to or above 1.4 D, and the keratometric difference between both eyes is above 1.0 D (sensitivity and specificity of 96% and 85%, respectively).[51,53–55]

The Maeda et al.[52] criteria allow keratoconus screening by analysis of the keratoconus index (KCI). A KCI value above 0% is codified as "similarity to keratoconus." This method has been shown to have an associated sensitivity and specificity for the detection of keratoconus of 98% and 99%, respectively. On the other hand, the keratoconus percentage index (KISA%) is a detection method derived from the topographic indexes that were originally created for analysis of the corneal surface with the TMS videokeratograph (Tomey Corp.).[55] It uses a combination of 4 topographic parameters: K value (defined as the weighted average of the paracentral dioptric value), I–S index, corneal toricity, and nonorthogonal corneal toricity value (SRAX).[51,55,56] The KISA% index is calculated as follows:

$$KISA\% = \frac{K \times I - S \times Cylinder \times SRAX \times 100}{300} \quad (1)$$

A value of KISA% index higher than 100 is classified as a susceptible pattern of keratoconus.[53,55]

The keratoconus prediction index (KPI) is another descriptor used as a clinical tool for keratoconus detection.[57] It is calculated as the combination of 7 topographic parameters characterizing the morphology of the anterior corneal surface: simulated keratometry (SimK), differential sector index (DSI), opposite sector index (OSI), center/surround index (CSI), SAI, irregular astigmatism index (IAI), and percent analyzed area (AA). The following formula is used for such calculation:

$$KPI = 0.30 + 0.01\begin{pmatrix} -41.23 - 0.15 \times DSI + 1.18 \times OSI + 1.49 \times CSI + 4.13 \times SAI - 0.60 \times SimK1 \\ +1.08 \times SimK2 - 3.74 \times IAI + 0.10 \times AA \end{pmatrix} \quad (2)$$

Values of this index above 0.38 can be considered as pathological, with a sensitivity of 86% and a specificity of 100%.[57]

Other specific descriptors of some corneal topography systems, such as those provided by the Scheimpflug-based Pentacam system (Oculus, Inc.) (anterior and posterior corneal topography analyzer, corneal aberrometer, pachymeter, and anterior segment biometer), are calculated according to proprietary algorithms:[58] index of surface variation (deviation of the corneal radius respect to the mean value), index of vertical asymmetry (characterization of the level of symmetry of curvature data relative to the horizontal meridian), keratoconus index, center keratoconus index, the smallest radius of curvature of the corneal area analyzed, index of height asymmetry (characterization of the level of symmetry of elevation data respect to the horizontal meridian), index of height decentration (estimation obtained from Fourier analysis), and aberration coefficient (estimation obtained from Zernike polynomials-based analysis). The abnormality ranges for all these parameters are shown in Table 2.

In addition to these approaches, numerous innovations have been developed to obtain more sensitive detection criteria, such as neural network approaches and specific mathematical models for reconstruction of the geometry of the anterior corneal surface.[7,8,59–63] The digital analysis of the image of the Placido disks projected on the cornea has also been shown to be a valid tool for keratoconus diagnosis, avoiding the use of estimated data or parameters obtained indirectly.[64] Specifically, the use of primary corneal indices characterizing the asymmetry of the mires seems to be especially useful for keratoconus detection.[64]

ANALYSIS OF THE POSTERIOR CORNEAL SURFACE IN KERATOCONUS

The elevation and curvature of the posterior corneal surface have been shown to be screening factors for

Table 2. Abnormality ranges for the topographic parameters provided by the Pentacam system.

Topographic Parameter	Suspicious	Pathological
Index of surface variation	≥ 0.37	≥ 41
Index of vertical asymmetry	≥ 0.28	≥ 0.32
Keratoconus index	> 1.07	> 1.07
Center keratoconus index	≥ 1.03	≥ 1.03
Smallest radius of curvature	< 6.71	< 6.71
Index of height asymmetry	≥ 19	> 21
Index of height decentration	≥ 0.014	> 0.016
Aberration coefficient	≥ 1	≥ 1

keratoconus.[14–16,20–22] Specifically, in keratoconus and also in keratoconus suspect, significantly larger values of BFS[14,16,21] and posterior elevation[15,16,22] have been reported (Figure 3). Schlegel et al.[16] report a mean aconic astigmatism for the posterior corneal surface of 2.29 D ± 1.71 (SD) in a sample of 48 keratoconus-suspect patients using scanning-slit technology. In the same sample, they also found a mean maximum posterior elevation of 0.0288 ± 0.0102 µm at 1.0 mm of radius from the center.[16] De Sanctis et al.[14] evaluated the diagnostic ability of maximum posterior corneal elevation measured in the 5.0 mm central zone with the Scheimpflug photography-based Pentacam system (anterior and posterior corneal topography analyzer, corneal aberrometer, pachymeter, and anterior segment biometer) in 75 patients with keratoconus and 25 eyes with subclinical keratoconus (keratoconus suspect by definition). They found the cutoff values of 35 µm (sensitivity 97.3%, specificity 96.9%) and 29 µm (sensitivity 68%, specificity 90.8%) for clinical and subclinical keratoconus, respectively. Fam and Lim[65] defined the posterior elevation ratio as the ratio of the maximum posterior elevation in the central 5.0 mm corneal zone to the BFS for the posterior cornea. They obtained a mean value for this ratio of 1.874 ± 0.532 in a sample of 43 keratoconus patients and of 1.103 ± 0.462 in a sample of 23 keratoconus suspects using scanning-slit technology.[65] In addition, they found excellent keratoconus detection ability of the same ratio obtained using the anterior elevation data (cutoff: 0.5122, sensitivity: 99%, specificity: 95.2%).[65]

Another tool used for keratoconus detection by some clinicians is the dioptric value of the BFS for the posterior corneal surface provided by the Orbscan system (scanning-slit technology) (anterior and posterior corneal topography analyzer, pachymeter, and anterior segment biometer). Posterior BFS values above 54.0 D should theoretically alert the examiner if the anterior BFS is within the normal range (41.0 to 46.0 D).[66] However, this dioptric value for the posterior corneal surface is not a real estimation because it is calculated assuming a change in refractive index at the posterior surface identical to that occurring at the anterior surface. Indeed, the posterior corneal curvature is always negative due to the refractive index change at this surface.[3]

CORNEAL ABERROMETRIC ANALYSIS IN KERATOCONUS

Anterior corneal aberration analysis has been proven to be an effective tool to detect and grade keratoconus (Figure 4).[2–6,17,67,68] Higher amounts of vertical coma and larger values of coma-like root mean square (RMS) have been reported in patients with keratoconus or keratoconus suspect.[2–6,17,67] In 2006, the first keratoconus severity grading system that used the magnitude of anterior corneal coma-like aberrations as the main classifying criterion was developed (Table 3).[4] In 23 eyes with keratoconus, 10 eyes with subclinical keratoconus (keratoconus suspect by definition), and 127 controls, Bühren et al.[17] evaluated the keratoconus detection ability of anterior corneal

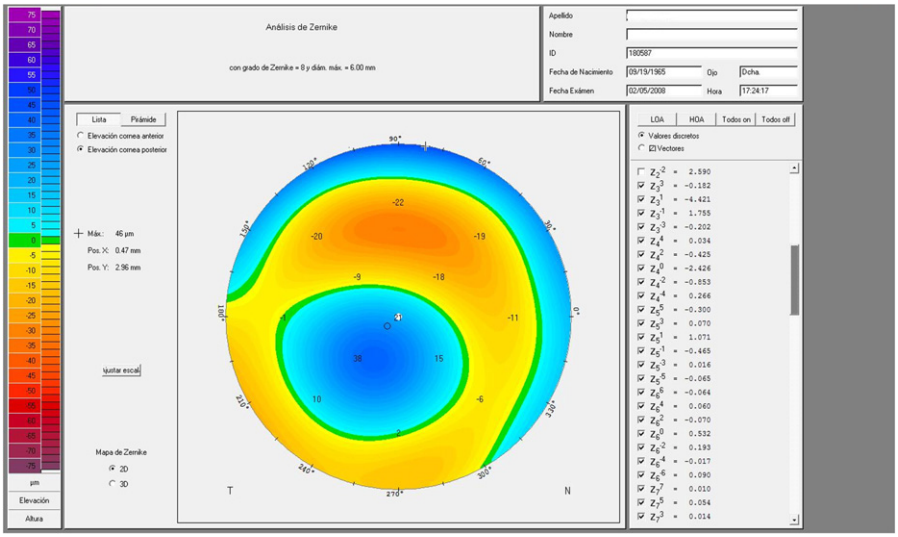

Figure 3. Tangential map of the posterior corneal surface obtained by the Pentacam Scheimpflug photography. In this keratoconic cornea, there is an I–S asymmetry in the posterior corneal surface that is similar to that normally found in the anterior corneal surface in keratoconus.

higher-order aberrations (HOAs). The found the cutoff points of 0.555 (sensitivity 100%, specificity 98.4%) and 0.248 µm (sensitivity 100%, specificity 73.6%) for clinical and subclinical keratoconus, respectively.[17]

In addition to anterior corneal aberrations, posterior corneal aberrometric data are useful for keratoconus diagnosis.[69,70] Nakagawa et al.[69] found large amounts of primary coma in the anterior and posterior corneal surfaces (primary coma RMS anterior/posterior: 3.57/0.87 µm) in 28 keratoconic eyes, although coma from the posterior surface compensated partly for that from the anterior surface. The Scheimpflug photography-based Pentacam system, (anterior and posterior corneal topography analyzer, corneal aberrometer, pachymeter, and anterior segment biometer) was the first commercially available topographer to provide an estimation of the wavefront aberrations of the posterior corneal surface, although with some limitations and inaccuracies.[3] Currently, accurate aberrometric analysis of the posterior cornea is provided by almost all Scheimpflug photography-based topography systems. It may be especially useful for the detection of keratoconus in its incipient stages, although some evidence demonstrates that posterior aberrations as well as thickness of the spatial profile do not markedly improve discriminative ability over that of anterior wavefront alone.[71]

It is preferable to use corneal wavefront aberrometry for keratoconus detection rather than total ocular aberration analysis. Total ocular aberrations (global aberrometry) are difficult if not impossible to measure accurately in highly aberrated eyes. Wavefront sensors that are available nowadays can analyze up to 1452 points maximum.[72] This sampling is limited for characterizing a very complex surface that induces large amounts of lower-order aberrations and HOAs. In addition, crowding or superimposing light spots or the assumption of flat slope of each analyzed portion of the wavefront, as happens with Hartmann-Shack devices, are features that limit the potential of

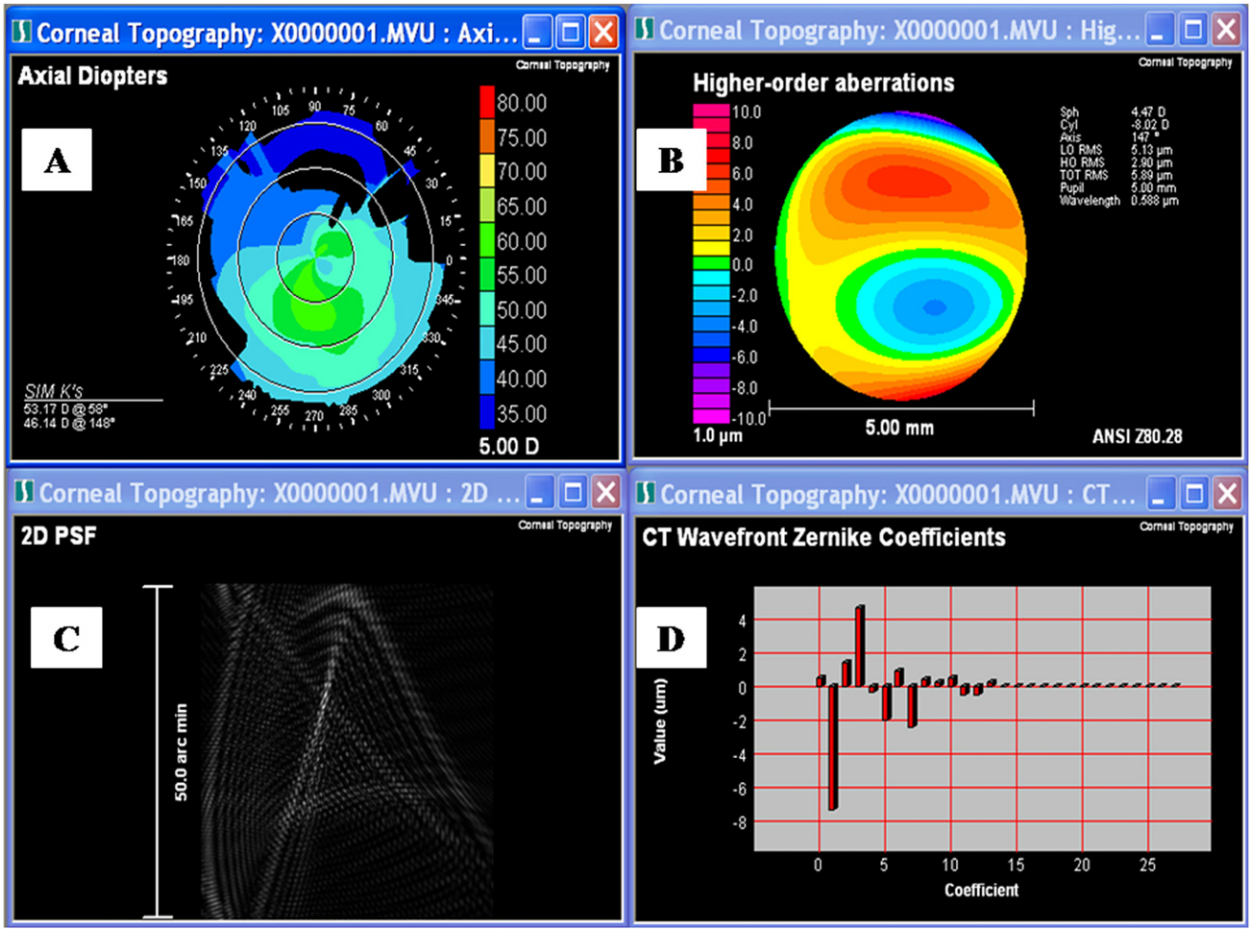

Figure 4. Aberrometric analysis (VOL-CT, version 6.20) of the anterior corneal surface in a keratoconic eye obtained by means of a Placido disk topography system. *A*: Placido-based axial corneal topography. *B*: Corneal higher-order wavefront map. *C*: The point spread function of the same keratoconic eye. *D*: Individual representation of each Zernike coefficient.

Table 3. Keratoconus grading system described by Alió and Shabayek[4] and based on anterior corneal coma-like aberrations (coma-like RMS) as the main classifying criterion.

Keratoconus Grade	Coma-like RMS *(μm)*	Other Features
1	1.50–2.50	No corneal scarring Mean central K < 48 D
2	> 2.50 ≤ 3.50	No corneal scarring Mean central K < 53 D Minimum corneal thickness > 400 μm
3	> 3.50 ≤ 4.50	No corneal scarring Mean central K > 53 D Minimum corneal thickness 200–400 μm
4	> 4.50	Corneal scarring Mean central K > 55 D Minimum corneal thickness 200 μm

K = keratometry; RMS = root mean square

analysis of these devices in keratoconus. With corneal topography systems, more than 6000 points can be studied and then a very exhaustive analysis can be performed without limitation to the pupillary area.[3] For all these reasons, corneal aberrometry has been established as a potential diagnostic tool for keratoconus.

PACHYMETRIC ANALYSIS IN KERATOCONUS

The pachymetric study, as well as the analysis of the corneal topographic pattern, is considered an indispensable tool in the preoperative screening of refractive surgery candidates and in diagnosing corneal ectasia.[73] Significant differences in central and minimum corneal thickness have been shown between subclinical, early, moderate, and advanced keratoconus, [67,74] which is useful to characterize the severity of keratoconus. The advances in imaging technology allow the clinician to obtain pachymetric maps providing point-by-point information of the entire cornea (Figure 5). A more detailed and accurate control of the progression of an ectatic disorder can be performed with these imaging advanced systems, such as those based on Scheimpflug photography, optical coherence tomographers, or very high-frequency ultrasonography systems (Figure 6).

In 46 eyes diagnosed with mild to moderate keratoconus and 364 normal eyes, Ambrósio et al.[24] evaluated the corneal thickness at the thinnest point and the averages of the points on 22 imaginary circles centered on the thinnest point with increased diameters at 0.4 mm steps using the Pentacam system and the Orbscan system (scanning-slit technology) (anterior and posterior corneal topography analyzer, pachymeter, and anterior segment biometer). They found statistically significant differences between groups in all positions of corneal-thickness spatial profile as well as in the percentage increase in thickness between 3.5 mm and 7.0 mm diameters.[24] These authors conclude that this pachymetric analysis could diagnose keratoconus and screen refractive candidates. In a study using the scanning-slit technology, Saad and Gatinel[75] found that indices generated from corneal thickness (percentage of thickness increase from the thinnest point to the periphery) and curvature measurements (percentage of variation of anterior and posterior curvatures) over the entire cornea centered on the thinnest point can identify very mild forms of ectasia undetected by a Placido-based neural network program. In a recent study by Ambrósio et al.[76] using the Pentacam technology, the tomographic-derived pachymetric parameters (pachymetric progression indices) were better factors to differentiate between normal and keratoconic corneas than single-point pachymetric measurements. Using a specific model of an optical coherence tomographer, Li et al.[77] found that pachymetric maps of 27 keratoconic eyes were more asymmetric (I–S, −44.8 ± 28.7 μm versus −9.9 ± 9.3 μm; cutoff, −31.3 μm; inferotemporal–superonasal, −63 ± 35.7 μm versus −22 ± 11.4 μm; cutoff, −48.2 μm) than maps corresponding to 34 controls evaluated. The cutoff points in this study had an associated sensitivity and specificity similar to KISA% index.[77]

Analysis of the epithelial thickness profile has also been shown to be useful for keratoconus detection and characterization.[78,79] Specifically, the presence of an underlying stromal cone seems to be associated with an epithelial doughnut pachymetric pattern. Therefore, this characteristic epithelial thickness doughnut may be considered a diagnostic test for keratoconus. However, it should be considered that epithelial compensation can mask the presence of an underlying cone in very early keratoconus.[78]

CORNEAL VOLUME ANALYSIS IN KERATOCONUS

Corneal volume was recently identified as an additional screening factor for keratoconus.[24,46,74,80,81] Significant differences in corneal volume have been reported between normal and moderate keratoconic eyes (Pentacam system: 60.83 ± 3.27 mm^3 controls versus 57.98 ± 2.65 mm^3 moderate keratoconus),[46] suggesting the potential role for corneal volume as a diagnostic factor for corneal ectatic disorders. However, there is not enough scientific evidence of the potential usefulness of corneal volume as a screening factor for keratoconus suspect.

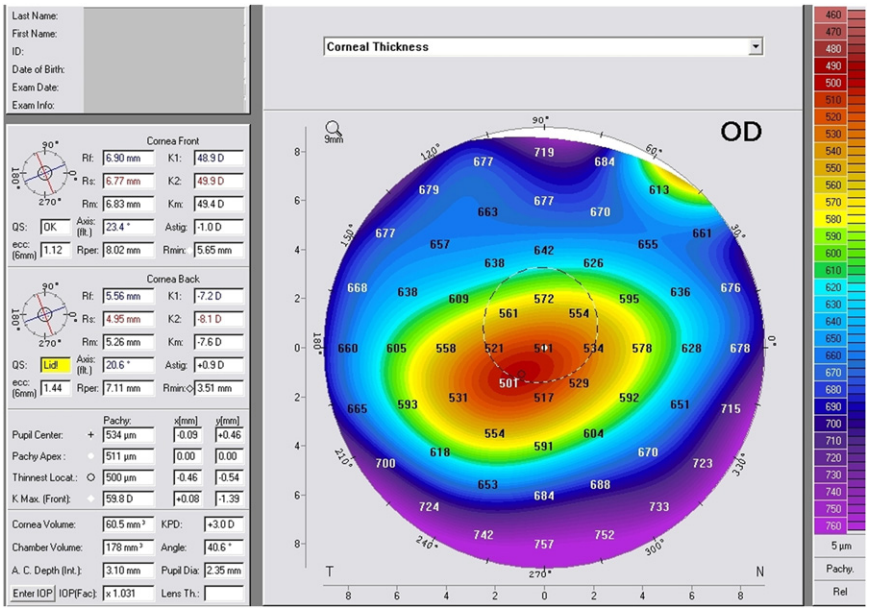

Figure 5. Pachymetric map of a keratoconic eye obtained by means of the Scheimpflug photography-based system.

CORNEAL BIOMECHANICS IN KERATOCONUS

As all the topographic and aberrometric alterations in keratoconic eyes are the consequence of the biomechanical changes in the corneal structure,[2] the study of corneal biomechanics has been proposed as an additional test for keratoconus diagnosis.[82,83] However, the in vivo evaluation of corneal biomechanical properties is not easy. To date, only one clinical device has been developed for characterizing the viscoplasticity of the cornea, the Ocular Response Analyzer (ORA) (Reichert, Inc.) (corneal biomechanics analyzer and air tonometer), which is based on analysis of the corneal reaction during a bidirectional applanation process.[84] Specifically, this device delivers an air pulse to the eye that causes the cornea to move inward, achieving a specific applanation state or flattening (Pressure 1). Milliseconds after the first applanation, the pressure decreases and the cornea passes through a second applanated state (Pressure 2) while returning from concavity to its normal convex curvature (Figure 7). The initial version of this instrument provided only 2 biomechanical parameters associated with this process: corneal hysteresis (CH) and the corneal

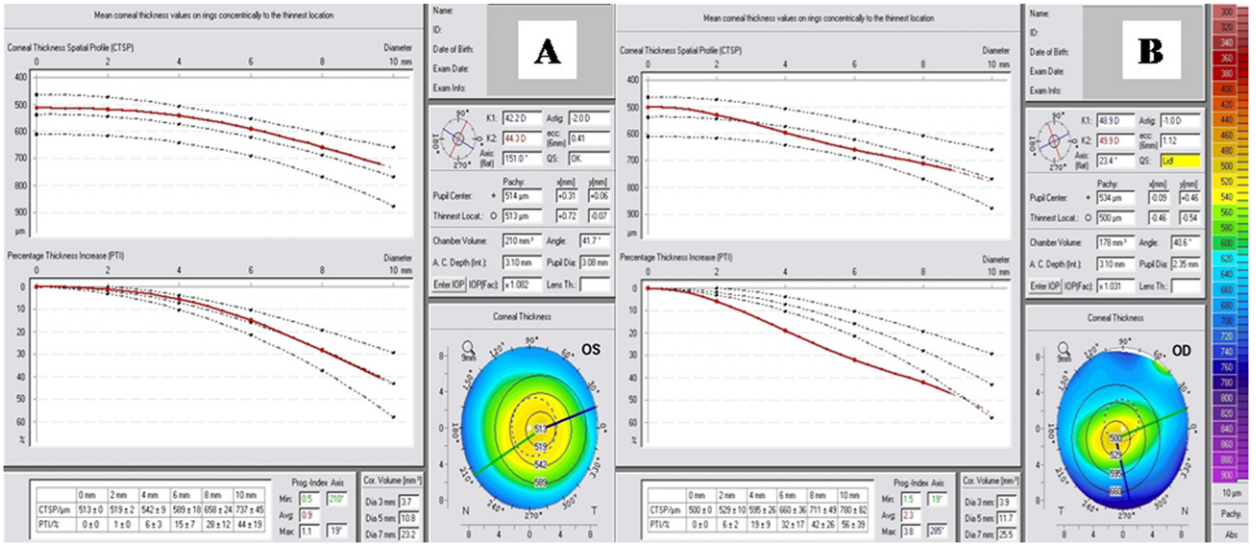

Figure 6. Module of pachymetric analysis from the Pentacam system. Normality ranges are provided for the increase in thickness from center to periphery. *A*: Normal cornea. *B*: Keratoconic cornea.

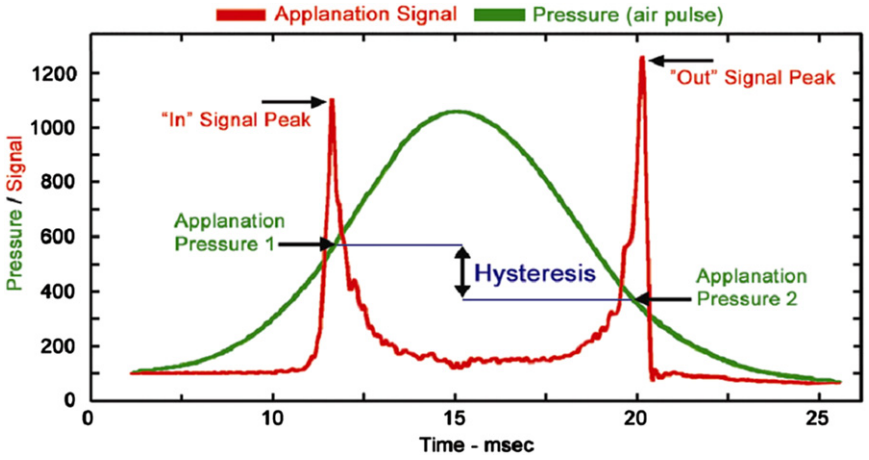

Figure 7. Signal diagram obtained with the ORA in a normal eye. The red line represents the applanation signal and the green line the pressure changes. As shown, the device delivers an air pulse to the eye, which causes the cornea to move inward achieving a specific applanation state or flattening (Pressure 1). Milliseconds after the first applanation, the pressure decreases and the cornea passes through a second applanated state (Pressure 2) while returning from concavity to the normal convex curvature.

resistance factor (CRF). Corneal hysteresis is defined as the difference between the 2 pressures (Pressures 1 and 2) recorded during the measurement process described. The CRF is calculated using a proprietary algorithm and is said to be predominantly related to the elastic properties of the cornea.[84] These parameters, CH and CRF, have been shown to be reproducible in nonoperated healthy eyes.[85]

Some authors have demonstrated that CH and CRF are significantly lower in keratoconic eyes than in normal eyes.[82,83] Ortiz et al.[83] compared the ORA outcomes in 165 normal eyes and 21 eyes with keratoconus (47% grade I according to the Amsler-Krumeich grading system), obtaining the mean values of 10.8 ± 1.5 mm Hg and 7.7 ± 1.3 mm Hg, respectively. The between-group difference was statistically significant. However, CH and CRF have been demonstrated as poor parameters for discriminating between mild keratoconus and normal corneas.[86] Specifically, Fontes et al.[86] performed a receiver operating characteristic curve analysis, obtaining a poor overall predictive accuracy of CH (cutoff, 9.64 mm Hg; sensitivity, 87%; specificity, 65%; test accuracy, 74.83%) and CRF (cutoff, 9.60 mm Hg; sensitivity, 90.5%; specificity, 66%; test accuracy, 76.97%) for detecting mild keratoconus. In addition, the CRF has been better than CH in detecting keratoconic corneas once the effect of central corneal thickness on ORA measurements is considered.[87] It should be noted that although the manufacturer states that the CH may primarily reflect corneal viscosity and the CRF may predominantly relate to the elastic properties of the cornea, the exact physical meaning of these parameters is not well understood. The parameters are said to represent the viscoelastic properties of the cornea, but no study proves whether these parameters are related to the standard mechanical properties used for describing the elastic materials (Young modulus).

To overcome the limited diagnostic performance of CH and CRF, new parameters based on the analysis of the response signal curve have been developed.[88] First results with this type of analysis are promising,[88] but more scientific evidence of its diagnostic value is required.

INTEGRAL ANALYSIS OF CORNEAL STRUCTURE

No clinical parameter provides 100% sensitivity and specificity for the detection of keratoconus, especially the subclinical forms. The combination of several clinical tests is extremely useful for detection and complete characterization of keratoconus.[67] It should be mentioned that anamnesis is crucial because some antecedents, such as the diagnosis of corneal ectasia in other members of the family, can alert the clinician. Some studies reveal the presence of topographic patterns compatible with keratoconus in family members of patients diagnosed with keratoconus, as well as in the fellow eyes of patients in whom keratoconus has been clinically diagnosed.[89–91] Therefore, new diagnostic criteria based on parameters obtained from different clinical examinations, not only analysis of the anterior corneal surface, are necessary, especially when the most incipient cases are to be detected. Recent research on keratoconus is focused on this aim, attempting to find multiple models for predicting the presence of the ectasia. Using logistic regression analysis, Uçakhan et al.[92] found that the combined analysis of anterior and posterior corneal power, elevation, and thickness data provided by a Scheimpflug device effectively discriminated between ectatic corneas and normal corneas. Kovacs et al.[93] observed that there was a threshold level of posterior corneal elevation (40 μm) and corneal thickness (450 μm) beyond which

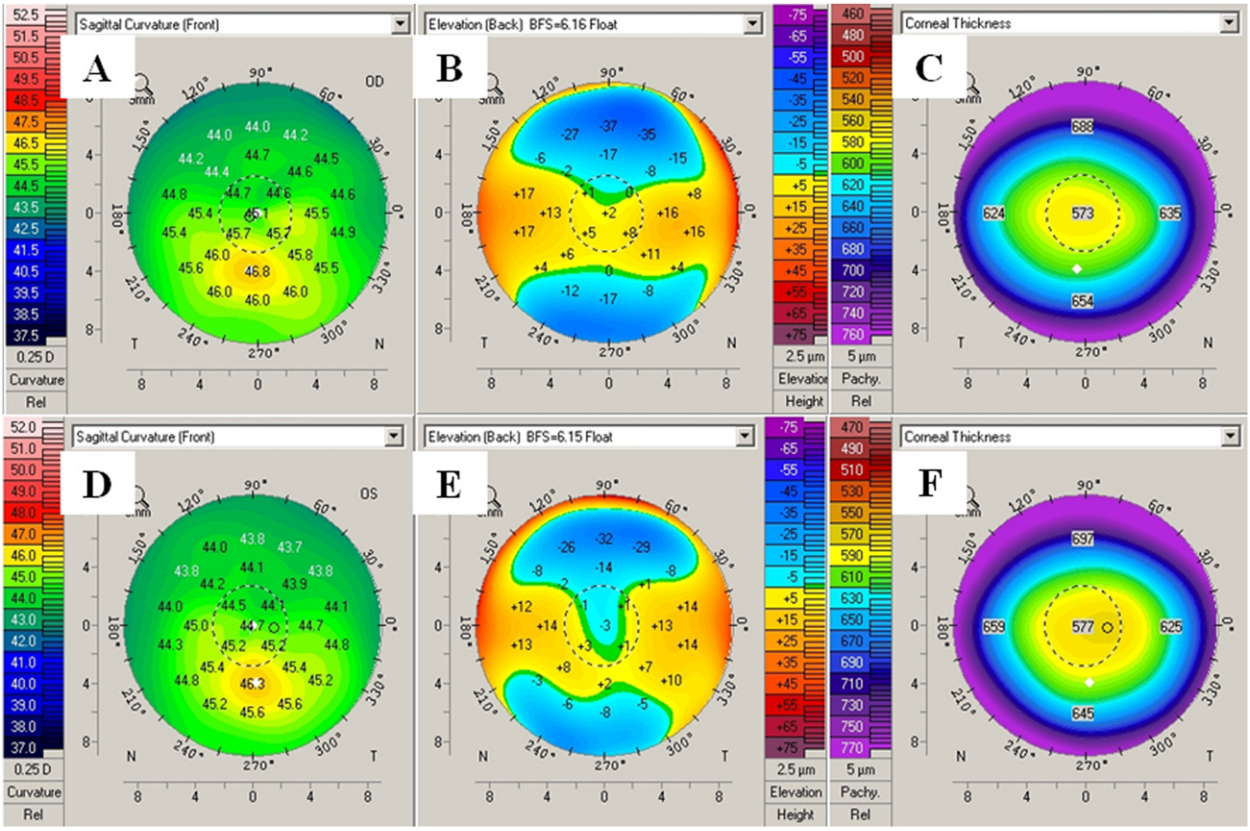

Figure 8. Keratoconus suspect topographical findings. *A* and *D*: Right eye (*RE*) and left eye (*LE*) sagittal maps show inferior steepening. *B* and *E*: Posterior elevation maps of both eyes do not show high elevation values. *C* and *F*: Pachymetry map values from both eyes are within normal limits.

the level of corneal protrusion in keratoconus accelerated. Alió et al.[67] found that the vectorial difference between refractive (calculated to the corneal plane) and corneal astigmatism was a relevant factor to include in predictive models for keratoconus detection (ocular residual astigmatism). Specifically, these authors

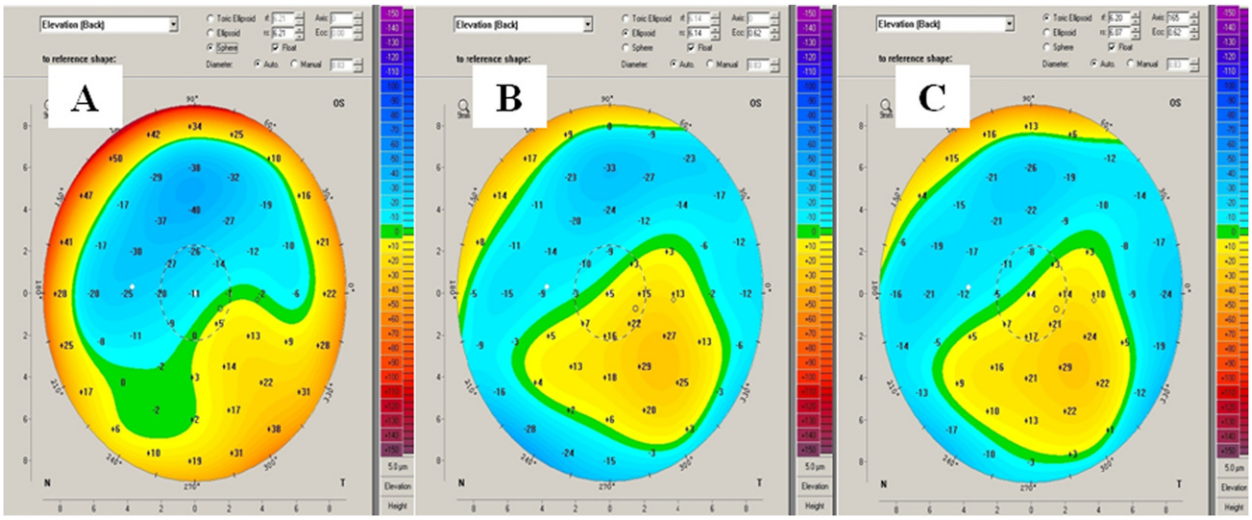

Figure 9. Appropriate selection of the reference surface is mandatory for an accurate diagnosis of an incipient ectasia. *A*: When the selected reference surface is a sphere, the map does not show values outside normal limits. *B*: If an ellipsoid is selected as reference surface, the elevation map shows suspicious values. C: Similarly, when a toric ellipsoid is chosen as reference surface, posterior elevation map again shows values associated with ectasia.

found a significantly higher magnitude of ocular residual astigmatism in keratoconic eyes showing more visual deterioration.[67]

KERATOCONUS SUSPECT

In the keratoconus suspect condition, the cornea does not show any typical alteration of a clinical keratoconus such as Munson sign, scissors-like retinoscopic reflex, asymmetric corneal thinning, Fleischer ring, or Vogt striae. Therefore, the keratoconus suspect cornea is apparently normal, except for the suspicious topographic signs that can be detected (Figure 8). As noted previously, anterior corneal topography is crucial for the diagnosis of keratoconus suspect: I–S index of 1.4 D or higher, hemimeridian angling higher than 20 degrees in relation to the vertical meridian, and inferior steepening.[94] Studying the posterior corneal surface using the elevation map also provides valuable information for detecting incipient states of ectatic disorders (Figure 9), as noted in a previous section. This type of examination may be especially useful in detecting very incipient keratoconus because hyperplasic activity of the corneal epithelium is able to mask subtle ectatic changes.

This type of ectasia constitutes a contraindication to laser in situ keratomileusis because the flap creation in conjunction with the excimer laser ablation might produce a biomechanical disorder that can trigger the mechanisms toward progressive forms.[95] For this reason, photorefractive keratectomy or laser-assisted subepithelial keratectomy has been presented as an adequate technique in keratoconus suspect patients, although the potential risk for iatrogenic ectasia is not completely eliminated.[96,97]

ATYPICAL FORMS OF KERATOCONUS

Although the most common keratoconus form is the presence of localized steepening over the inferior midperipheral zone, cases of superior keratoconus have been reported.[98,99] The characteristic topographic pattern is similar to that corresponding to classic keratoconus but with the localized steepening located above the horizontal meridian.

Posterior keratoconus consists of a central or paracentral depression in the posterior corneal surface with an intact but abnormal Descemet membrane.[100] Two forms of posterior keratoconus can be differentiated according to the extent of the area of the posterior corneal surface that is affected: the entire posterior corneal curvature (keratoconus posticus totalis) or a localized portion (keratoconus posticus circumscriptus).[101,102] It is an uncommon, noninflammatory, and nonprogressive corneal disease that is normally unilateral. Posterior keratoconus is usually detected during a routine ophthalmologic examination when moderate amblyopia or irregular retinoscopic reflexes are observed. In these cases, the anterior corneal surface is not altered, although Mannis et al.[102] also observed specific abnormalities in this surface.

PSEUDOKERATOCONUS: ARTIFACTS IN THE CHARACTERIZATION OF CORNEAL STRUCTURE

Some acquisition artifacts with currently available corneal topography systems can lead to errors in interpretation of the measurements by the topographer software. Some of these errors consist of the detection of unreal corneal surfaces susceptible of being interpreted by the clinician as keratoconic or suspicious of keratoconus (pseudokeratoconus). The following are factors that can induce this type of artifact:

Incorrect patient positioning during measurement: The correct patient position during the topographic acquisition as well as the correct eye alignment with the fixation stimulus is crucial to obtain repeatable and clinically useful topographic data. Eyelids under continuing pressure from different gaze positions have been shown to influence anterior corneal shape.[103] In addition, patients showing normal videokeratographies with a symmetrical bowtie pattern might show altered videokeratographies after some eye movements (Figure 10).

Contact lens–induced corneal warpage: Contact lens wear, especially with rigid gas-permeable lenses, might significantly alter corneal topographic patterns. Rigid gas-permeable lenses should be considered to have a higher rigidity module, and their bearing on the cornea can cause some transitory effect. This is the reason for asking contact lens wearers to discontinue use of the lenses at least 3 weeks before refractive surgery screening to obtain information of the corneal basal state (Figure 11).[104]

Tear-film stability and dry eye: Tear-film alterations constitute one of the most important factors for inducing the presence of artifacts in a topographic examination. A low tear film quality (low breakup time) or quantity (low Schirmer test values) might generate the presence of alterations in the anterior corneal surface such as epitheliopathies that can contribute to obtaining altered topographic patterns (Figure 12).[105] For all these factors, it is recommended that topographic acquisition be performed after an eye blink and that the consistency of measurement in cases of dry eye be confirmed by taking 3 consecutive measurements and comparing them.

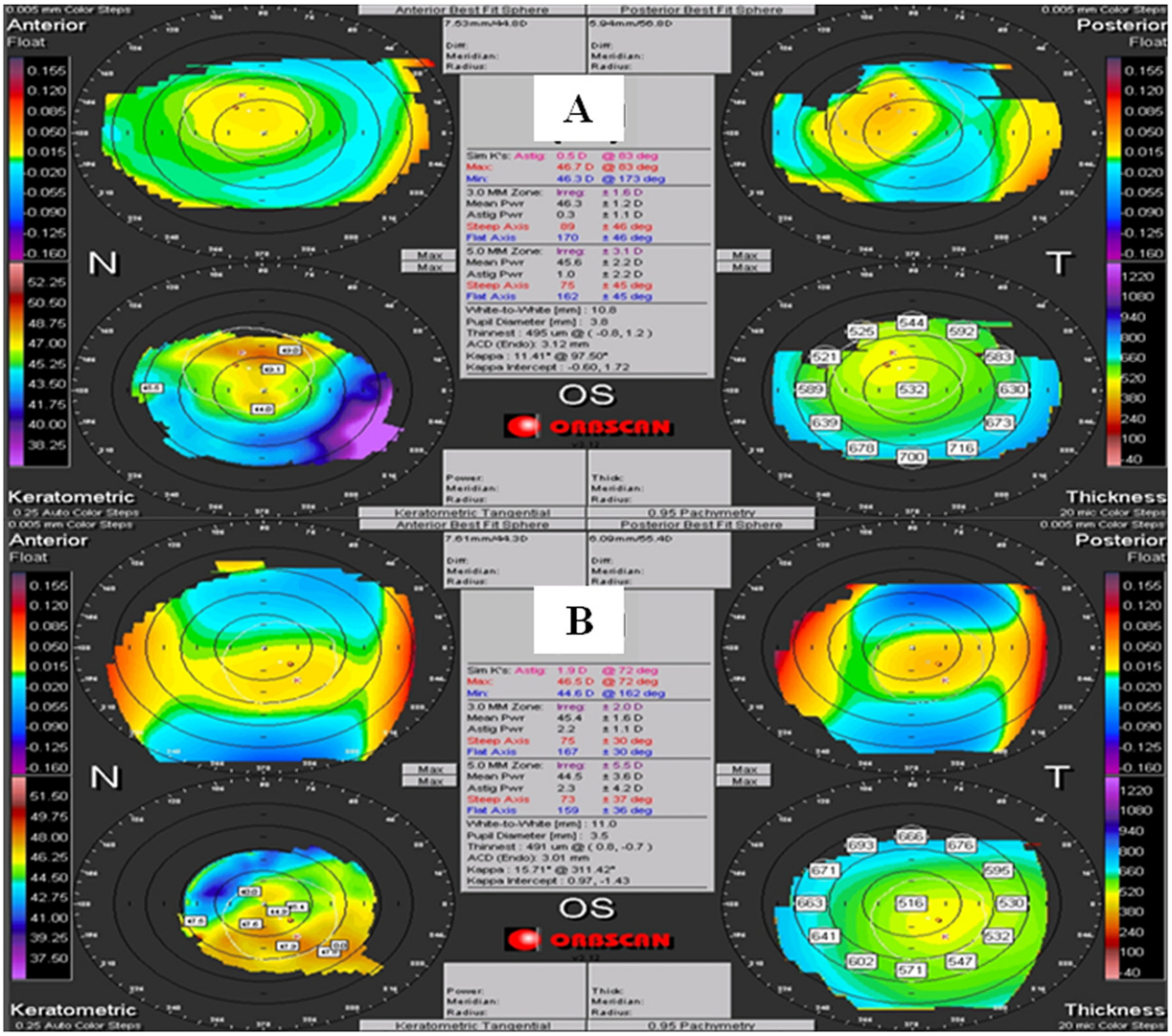

Figure 10. Appropriate alignment during acquisition is mandatory to avoid misdiagnosis. *A*: Topography map in supraversion eye position. *B*: Topography map in infraversion eye position. It looks similar to an inferior steepening that might mislead the diagnosis.

In conclusion, the following key points can be extracted from this review:

Combined analysis of anterior and posterior corneal power, elevation, and pachymetry data provides efficient discrimination between normal and ectatic corneas and a proper profound analysis for keratoconus follow-up purposes.

The use of tangential maps having adequate dioptric power steps is necessary for a high-quality corneal ectasia detection process when performing topographical analysis because erroneous selection might mislead decision-making procedures.

Numerous helpful topographic indexes and descriptors have been developed to characterize corneal shape. Clinicians should be familiar with the indexes provided by the ophthalmic devices commonly used during their daily clinics.

Wavefront analysis has recently been incorporated into the common screening test battery in outpatient eye clinics; thus, this technology might also be a valuable tool when diagnosing ectatic corneas. Other new cutting-edge technological analyses such as corneal volume assessment might be future screening factors that can be incorporated into the clinical practice.

Finally, accurate detection of subclinical or forme-fruste keratoconus is mandatory when counseling corneal refractive surgery candidates. Similarly, elimination of image acquisition artifacts during diagnostic procedures is obligatory to avoid misleading diagnoses.

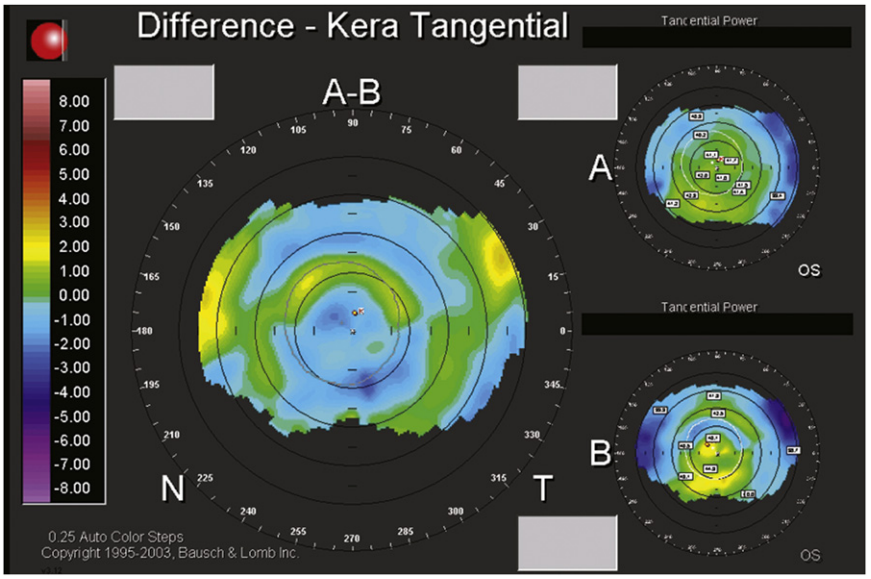

Figure 11. Differential keratometric map between the topography taken after 1 week (*B*) and 6 weeks (*A*) of RGP contact lens removal. A central cornea flattening has occurred after the RGP contact lens removal.

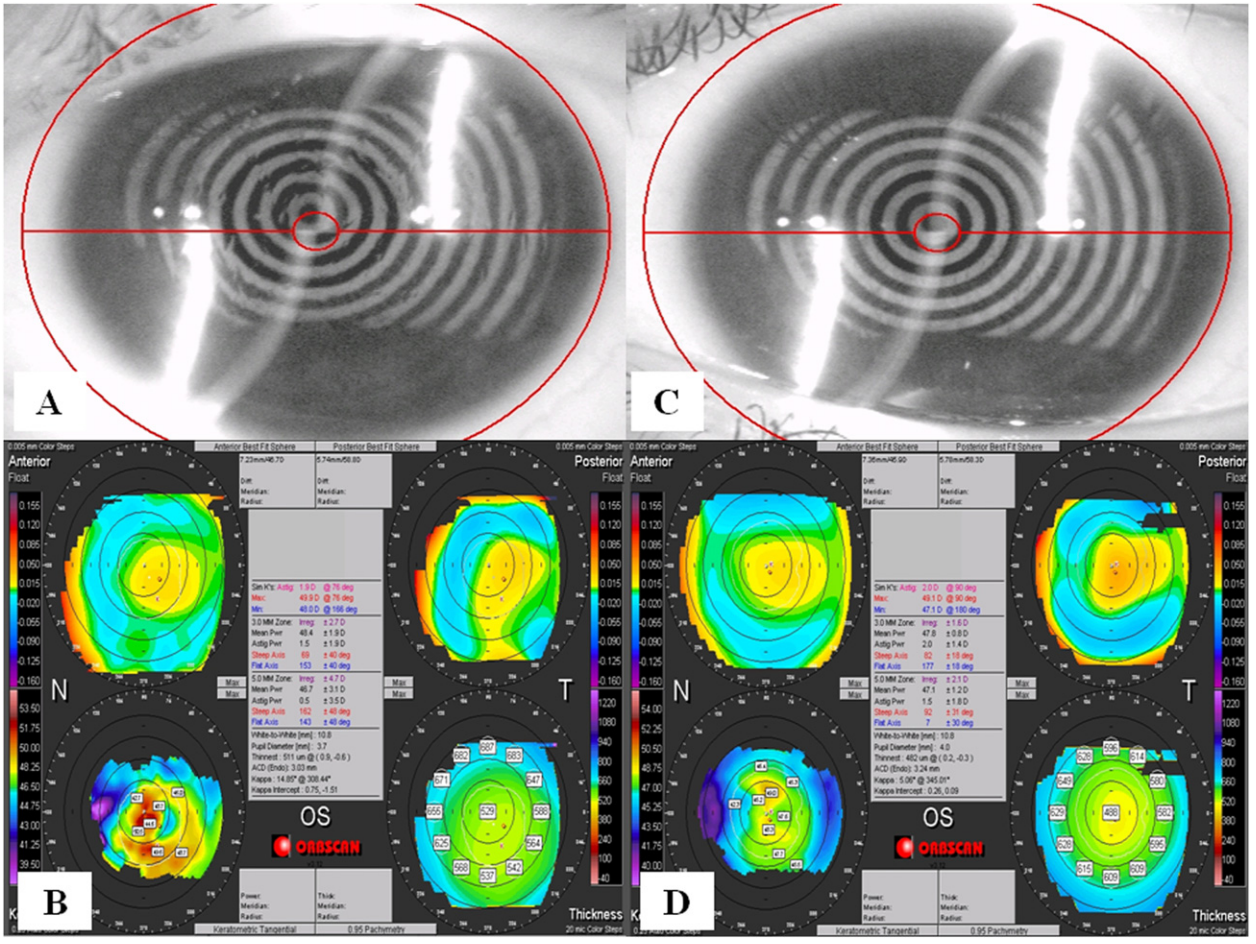

Figure 12. Tear-film breakup must be avoided during acquisition. *A*: Placido disk image shows irregularity while performing noninvasive breakup time test. *B*: Topography corresponding to image *A*. *C*: Homogeneous Placido disk image after preservative-free eyedrops instillation. *D*: Topography corresponding to image *C*.

REFERENCES

1. Rabinowitz YS. Keratoconus. Surv Ophthalmol 1998; 42:297–319. Available at: http://www.keratoconus.com/resources/Major+Review-Keratoconus.pdf. Accessed May 11, 2012
2. Piñero DP, Alió JL, Barraquer RI, Michael R, Jiménez R. Corneal biomechanics, refraction, and corneal aberrometry in keratoconus: an integrated study. Invest Ophthalmol Vis Sci 2010; 51:1948–1955. Available at: http://www.iovs.org/content/51/4/1948.full.pdf. Accessed May 11, 2012
3. Piñero DP, Alió JL, Alesón A, Escaf M, Miranda M. Pentacam posterior and anterior corneal aberrations in normal and keratoconic eyes. Clin Exp Optom 2009; 92:297–303. Available at: http://onlinelibrary.wiley.com/doi/10.1111/j.1444-0938.2009.00357.x/pdf. Accessed May 11, 2012
4. Alió JL, Shabayek MH. Corneal higher order aberrations: a method to grade keratoconus. J Refract Surg 2006; 22:539–545
5. Gobbe M, Guillon M. Corneal wavefront aberration measurements to detect keratoconus patients. Contact Lens Anterior Eye 2005; 28:57–66
6. Barbero S, Marcos S, Merayo-Lloves J, Moreno-Barriuso E. Validation of the estimation of corneal aberrations from videokeratography in keratoconus. J Refract Surg 2002; 18:263–270
7. Carvalho LA. Preliminary results of neural networks and Zernike polynomials for classification of videokeratography maps. Optom Vis Sci 2005; 82:151–158. Available at: http://journals.lww.com/optvissci/Fulltext/2005/02000/Absolute_Accuracy_of_Placido_Based.15.aspx. Accessed May 11, 2012
8. Accardo PA, Pensiero S. Neural network-based system for early keratoconus detection from corneal topography. J Biomed Inform 2002; 35:151–159
9. Holladay JT. Corneal topography using the Holladay Diagnostic Summary. J Cataract Refract Surg 1997; 23:209–221
10. Borderie VM, Laroche L. Measurement of irregular astigmatism using semimeridian data from videokeratographs. J Refract Surg 1996; 12:595–600
11. Kalin NS, Maeda N, Klyce SD, Hargrave S, Wilson SE. Automated topographic screening for keratoconus in refractive surgery candidates. CLAO J 1996; 22:164–167
12. Rabinowitz YS, McDonnell PJ. Computer-assisted corneal topography in keratoconus. Refract Corneal Surg 1989; 5:400–408
13. Dingeldein SA, Klyce SD, Wilson SE. Quantitative descriptors of corneal shape derived from computer-assisted analysis of photokeratographs. Refract Corneal Surg 1989; 5:372–378
14. De Sanctis U, Loiacono C, Richiardi L, Turco D, Mutani B, Grignolo FM. Sensitivity and specificity of posterior corneal elevation measured by Pentacam in discriminating keratoconus/subclinical keratoconus. Ophthalmology 2008; 115:1534–1539
15. Nilforoushan M-R, Speaker M, Marmor M, Abramson J, Tullo W, Morschauser D, Latkany R. Comparative evaluation of refractive surgery candidates with Placido topography, Orbscan II, Pentacam, and wavefront analysis. J Cataract Refract Surg 2008; 34:623–631
16. Schlegel Z, Hoang-Xuan T, Gatinel D. Comparison of and correlation between anterior and posterior corneal elevation maps in normal eyes and keratoconus-suspect eyes. J Cataract Refract Surg 2008; 34:789–795
17. Bühren J, Kühne C, Kohnen T. Defining subclinical keratoconus using corneal first-surface higher-order aberrations. Am J Ophthalmol 2007; 143:381–389
18. Jafri B, Li X, Yang H, Rabinowitz YS. Higher order aberrations and topography in early and suspected keratoconus. J Refract Surg 2007; 23:774–781
19. Lim L, Wei RH, Chan WK, Tan DTH. Evaluation of higher order ocular aberrations in patients with keratoconus. J Refract Surg 2007; 23:825–828
20. Tomidokoro A, Oshika T, Amano S, Higaki S, Maeda N, Miyata K. Changes in anterior and posterior corneal curvatures in keratoconus. Ophthalmology 2000; 107:1328–1332
21. Sonmez B, Doan M-P, Hamilton DR. Identification of scanning slit-beam topographic parameters important in distinguishing normal from keratoconic corneal morphologic features. Am J Ophthalmol 2007; 143:401–408
22. Rao SN, Raviv T, Majmudar PA, Epstein RJ. Role of Orbscan II in screening keratoconus suspects before refractive corneal surgery. Ophthalmology 2002; 109:1642–1646
23. Swartz T, Marten L, Wang M. Measuring the cornea: the latest developments in corneal topography. Curr Opin Ophthalmol 2007; 18:325–333. Available at: http://www.v2020la.org/pub/PUBLICATIONS_BY_TOPICS/Cornea/Measuring%20the%20cornea.pdf. Accessed May 11, 2012
24. Ambrósio R Jr, Alonso RS, Luz A, Coca Velarde LG. Corneal-thickness spatial profile and corneal-volume distribution: tomographic indices to detect keratoconus. J Cataract Refract Surg 2006; 32:1851–1859
25. Sharma V, Sharma N, Vajpayee RB, Titiyal JS, Sinha R. Study of corneal topographic patterns with single continuous suturing techniques in penetrating keratoplasty. Cornea 2003; 22:5–9
26. Bogan SJ, Waring GO III, Ibrahim O, Drews C, Curtis L. Classification of normal corneal topography based on computer-assisted videokeratography. Arch Ophthalmol 1990; 108:945–949. Available at: http://archopht.ama-assn.org/cgi/reprint/108/7/945. Accessed May 11, 2012
27. Alvi NP, McMahon TT, Devulapally J, Cheng TC, Vianna MA. Characteristics of normal corneal topography using the EyeSys corneal analysis system. J Cataract Refract Surg 1997; 23:849–855
28. Naufal SC, Hess JS, Friendlander MH, Granet NS. Rasterstereography-based classification of normal corneas. J Cataract Refract Surg 1997; 23:222–230
29. Rabinowitz YS, Yang H, Brickman Y, Akkina J, Riley C, Rotter JI, Elashoff J. Videokeratography database of normal human corneas. Br J Ophthalmol 1996; 80:610–616. Available at: http://www.ncbi.nlm.nih.gov/pmc/articles/PMC505554/pdf/brjopthal00007-0030.pdf. Accessed May 11, 2012
30. Wilson SE, Lin DTC, Klyce SD. Corneal topography of keratoconus. Cornea 1991; 10:2–8
31. Auffarth GU, Wang L, Völcker HE. Keratoconus evaluation using the Orbscan Topography System. J Cataract Refract Surg 2000; 26:222–228
32. Bafna S, Kohnen T, Koch DD. Axial, instantaneous, and refractive formulas in computerized videokeratography of normal corneas. J Cataract Refract Surg 1998; 24:1184–1190
33. Szczotka LB, Thomas J. Comparison of axial and instantaneous videokeratographic data in keratoconus and utility in contact lens curvature prediction. CLAO J 1998; 24:22–28
34. Rabinowitz YS. Tangential vs sagittal videokeratographs in the "early" detection of keratoconus. Am J Ophthalmol 1996; 122:887–889
35. Roberts C. Analysis of the inherent error of the TMS-1 Topographic Modeling System in mapping a radially aspheric surface. Cornea 1995; 14:258–265
36. Chan JS, Mandell RB, Burger DS, Fusaro RE. Accuracy of videokeratography for instantaneous radius in keratoconus. Optom Vis Sci 1995; 72:793–799
37. Characterization of the inherent error in a spherically-biased corneal topography system in mapping a radially aspheric surface. J Refract Corneal Surg 1994; 10:103–111; discussion by RB Mandell, RA Applegate & reply by C Roberts, 112–116

38. Smolek MK, Klyce SD, Hovis JK. The Universal Standard Scale; proposed improvements to the American National Standards Institute (ANSI) scale for corneal topography. Ophthalmology 2002; 109:361–369
39. American National Standards Institute, Inc. American National Standard for Ophthalmics – Corneal Topography Systems - Standard Terminology, Requirements. New York, NY, ANSI Z80.23–1999
40. Wilson SE, Klyce SD, Husseini ZM. Standarized color-coded maps for corneal topography. Ophthalmology 1993; 100:1723–1727
41. González-Méijome JM, Villa-Collar C, Montés-Micó R, Gomes A. Asphericity of the anterior human cornea with different corneal diameters. J Cataract Refract Surg 2007; 33:465–473
42. Davis WR, Raasch TW, Lynn Mitchell G, Mutti DO, Zadnik K. Corneal asphericity and apical curvature in children: a cross-sectional and longitudinal evaluation. Invest Ophthalmol Vis Sci 2005; 46:1899–1906. Available at: http://www.iovs.org/content/46/6/1899.full.pdf. Accessed May 11, 2012
43. Clark B. Mean topography of the normal corneas. Aust J Optom 1974; 57:107–114
44. Mandell RB, St. Helen R. Mathematical model of the corneal contour. Br J Physiol Opt 1971; 26:183–197
45. Yebra-Pimentel E, González-Méijome JM, Cerviño A, Giráldez MJ, González-Pérez J, Parafita MA. Asfericidad corneal en una población de adultos jóvenes. Implicaciones clínicas [Corneal asphericity in a young adult population. Clinical implications]. Arch Soc Esp Oftalmol 2004; 79:385–392
46. Piñero DP, Alió JL, Alesón A, Escaf Vergara M, Miranda M. Corneal volume, pachymetry, and correlation of anterior and posterior corneal shape in subclinical and different stages of clinical keratoconus. J Cataract Refract Surg 2010; 36:814–825
47. Hansen DW. Evaluating the eye with corneal topography. Contact Lens Spectrum 2003; 18(8):27–32. Available at: http://www.clspectrum.com/articleviewer.aspx?articleID=12399. Accessed May 11, 2012
48. Wilson SE, Klyce SD. Quantitative descriptors of corneal topography; a clinical study. Arch Ophthalmol 1991; 109:349–353. Available at: http://archopht.ama-assn.org/cgi/reprint/109/3/349. Accessed May 11, 2012
49. Abad JC, Rubinfeld RS, Del Valle M, Belin MW, Kurstin JM. Vertical D; a novel topographic pattern in some keratoconus suspects. Ophthalmology 2007; 114:1020–1026
50. Shiotani Y, Maeda N, Inoue T, Watanabe H, Inoue Y, Shimomura Y, Tano Y. Comparison of topographic indices that correlate with visual acuity in videokeratography. Ophthalmology 2000; 107:559–564
51. Rabinowitz YS. Videokeratographic indices to aid in screening for keratoconus. J Refract Surg 1995; 11:371–379
52. Maeda N, Klyce SD, Smolek MK, Thompson HW. Automated keratoconus screening with corneal topography analysis. Invest Ophthalmol Vis Sci 1994; 35:2749–2757. Available at: http://www.iovs.org/cgi/reprint/35/6/2749.pdf. Accessed May 11, 2012
53. Rabinowitz YS, Rasheed K. KISA% index: a quantitative videokeratography algorithm embodying minimal topographic criteria for diagnosing keratoconus. J Cataract Refract Surg 1999; 25:1327–1335; errata, 2000; 26:480
54. Rabinowitz YS. Corneal topography. Curr Opin Ophthalmol 1995; 6:57–62
55. Twa MD, Parthasarathy S, Roberts C, Mahmood AM, Raasch TW, Bullimore MA. Automated decision tree classification of corneal shape. Optom Vis Sci 1995; 82:1038–1046. Available at: http://www.ncbi.nlm.nih.gov/pmc/articles/PMC3073139/pdf/nihms275710.pdf. Accessed May 11, 2012
56. Maeda N, Klyce SD, Smolek MK. Comparison of methods for detecting keratoconus using videokeratography. Arch Ophthalmol 1995; 113:870–874
57. Smolek MK, Klyce SD. Current keratoconus detection methods compared with a neural network approach. Invest Ophthalmol Vis Sci 1997; 38:2290–2299. Available at: http://www.iovs.org/cgi/reprint/38/11/2290. Accessed May 11, 2012
58. Kopacz D, Maciejewicz P, Keçik D. [The use of Pentacam for keratoconus diagnosis and progress evaluation] [Polish]. Klin Oczna 2011; 113:75–81
59. Martinez-Finkelshtein A, Delgado AM, Castro GM, Zarzo A, Alió JL. Comparative analysis of some modal reconstruction methods of the shape of the cornea from corneal elevation data. Invest Ophthalmol Vis Sci 2009; 50:5639–5645. Available at: http://www.iovs.org/content/50/12/5639.full.pdf. Accessed May 11, 2012
60. Yoon G, Pantanelli S, MacRae S. Comparison of Zernike and Fourier wavefront reconstruction algorithms in representing corneal aberration of normal and abnormal eyes. J Refract Surg 2008; 24:582–590
61. Carvalho LA. Accuracy of Zernike polynomials in characterizing optical aberrations and the corneal surface of the eye. Invest Ophthalmol Vis Sci 2005; 46:1915–1926. Available at: http://www.iovs.org/cgi/reprint/46/6/1915. Accessed May 11, 2012
62. Smolek MK, Klyce SD. Goodness-of-prediction of Zernike polynomials fitting to corneal surfaces. J Cataract Refract Surg 2005; 31:2350–2355
63. Iskander DR, Collins MJ, Davis B. Optimal modeling of corneal surfaces with Zernike polynomials. IEEE Trans Biomed Eng 2001; 48:87–95. Available at: http://eprints.qut.edu.au/762/1/58_-_Iskander_Collins_Davis01.pdf. Accessed May 11, 2012
64. Ramos-López D, Martínez-Finkelshtein A, Castro-Luna GM, Piñero D, Alió JL. Placido-based indices of corneal irregularity. Optom Vis Sci 2011; 88:1220–1231
65. Fam H-B, Lim K-L. Corneal elevation indices in normal and keratoconic eyes. J Cataract Refract Surg 2006; 32:1281–1287
66. Arntz A, Durán JA, Pijoán JI. Diagnóstico del queratocono subclínico por topografía de elevación [Subclinical keratoconus diagnosis by elevation topography]. Arch Soc Esp Oftalmol 2003; 78:659–664
67. Alió JL, Piñero DP, Alesón A, Teus MA, Barraquer RI, Murta J, Maldonado MJ, Castro de Luna G, Gutiérrez R, Villa C, Uceda-Montanes A. Keratoconus-integrated characterization considering anterior corneal aberrations, internal astigmatism, and corneal biomechanics. J Cataract Refract Surg 2011; 37:552–568
68. Applegate RA, Hilmantel G, Howland HC, Tu EY, Starck T, Zayac EJ. Corneal first surface optical aberrations and visual performance. J Refract Surg 2000; 16:507–514
69. Nakagawa T, Maeda N, Kosaki R, Hori Y, Inoue T, Saika M, Mihashi T, Fujikado T, Tano Y. Higher-order aberrations due to the posterior corneal surface in patients with keratoconus. Invest Ophthalmol Vis Sci 2009; 50:2660–2665. Available at: http://www.iovs.org/content/50/6/2660.full.pdf. Accessed May 11, 2012
70. Chen M, Yoon G. Posterior corneal aberrations and their compensation effects on anterior corneal aberrations in keratoconic eyes. Invest Ophthalmol Vis Sci 2008; 49:5645–5652. Available at: http://www.iovs.org/content/49/12/5645.full.pdf. Accessed May 11, 2012
71. Bühren J, Kook D, Yoon G, Kohnen T. Detection of subclinical keratoconus by using corneal anterior and posterior surface aberrations and thickness spatial profiles. Invest Ophthalmol Vis Sci 2010; 51:3424–3432. Available at: http://www.iovs.org/content/51/7/3424.full.pdf. Accessed May 11, 2012

72. Rozema JJ, Van Dyck DEM, Tassignon M-J. Clinical comparison of 6 aberrometers. Part 1: technical specifications. J Cataract Refract Surg 2005; 31:1114–1127
73. Ambrósio R Jr, Klyce SD, Wilson SE. Corneal topographic and pachymetric screening of keratorefractive patients. J Refract Surg 2003; 19:24–29
74. Emre S, Doganay S, Yologlu S. Evaluation of anterior segment parameters in keratoconic eyes measured with the Pentacam system. J Cataract Refract Surg 2007; 33:1708–1712
75. Saad A, Gatinel D. Topographic and tomographic properties of forme fruste keratoconus corneas. Invest Ophthalmol Vis Sci 2010; 51:5546–5555. Available at: http://www.iovs.org/content/51/11/5546.full.pdf. Accessed May 11, 2012
76. Ambrósio R Jr, Caiado ALC, Guerra FP, Louzada R, Roy AS, Luz A, Dupps WJ, Belin MW. Novel pachymetric parameters based on corneal tomography for diagnosing keratoconus. J Refract Surg 2011; 27:753–758
77. Li Y, Meisler DM, Tang M, Lu ATH, Thakrar V, Reiser BJ, Huang D. Keratoconus diagnosis with optical coherence tomography pachymetry mapping. Ophthalmology 2008; 115:2159–2166
78. Reinstein DZ, Archer TJ, Gobbe M. Corneal epithelial thickness profile in the diagnosis of keratoconus. J Refract Surg 2009; 25:604–610
79. Haque S, Jones L, Simpson T. Thickness mapping of the cornea and epithelium using optical coherence tomography. Optom Vis Sci 2008; 85:E963–E976. Available at: http://journals.lww.com/optvissci/Fulltext/2008/10000/Contrast_Sensitivity_Function_in_Patients_with.14.aspx. Accessed May 11, 2012
80. Mannion LS, Tromans C, O'Donnell C. Reduction in corneal volume with severity of keratoconus. Curr Eye Res 2011; 36:522–527
81. Cerviño A, Gonzalez-Meijome JM, Ferrer-Blasco T, Garcia-Resua C, Montes-Mico R, Parafita M. Determination of corneal volume from anterior topography and topographic pachymetry: application to healthy and keratoconic eyes. Ophthalmic Physiol Opt 2009; 29:652–660
82. Shah S, Laiquzzaman M, Bhojwani R, Mantry S, Cunliffe I. Assessment of the biomechanical properties of the cornea with the Ocular Response Analyzer in normal and keratoconic eyes. Invest Ophthalmol Vis Sci 2007; 48:3026–3031. Available at: http://www.iovs.org/cgi/reprint/48/7/3026. Accessed May 11, 2012
83. Ortiz D, Piñero D, Shabayek MH, Arnalich-Montiel F, Alió JL. Corneal biomechanical properties in normal, post-laser in situ keratomileusis, and keratoconic eyes. J Cataract Refract Surg 2007; 33:1371–1375
84. Luce DA. Determining in vivo biomechanical properties of the cornea with an ocular response analyzer. J Cataract Refract Surg 2005; 31:156–162
85. Moreno-Montañés J, Maldonado MJ, García N, Mendiluce L, García-Gómez P, Seguí-Gómez M. Reproducibility and clinical relevance of the Ocular Response Analyzer in nonoperated eyes: corneal biomechanical and tonometric implications. Invest Ophthalmol Vis Sci 2008; 49:968–974. Available at: http://www.iovs.org/cgi/reprint/49/3/968. Accessed May 11, 2012
86. Fontes BM, Ambrósio R Jr, Jardim D, Velarde GC, Nosé W. Corneal biomechanical metrics and anterior segment parameters in mild keratoconus. Ophthalmology 2010; 117:673–679
87. Galletti JG, Pförtner T, Bonthoux FF. Improved keratoconus detection by ocular response analyzer testing after consideration of corneal thickness as a confounding factor. J Refract Surg 2012; 28:202–208
88. Touboul D, Bénard A, Mahmoud AM, Gallois A, Colin J, Roberts CJ. Early biomechanical keratoconus pattern measured with an ocular response analyzer: curve analysis. J Cataract Refract Surg 2011; 37:2144–2150
89. Levy D, Hutchings H, Rouland JF, Guell J, Burillon C, Arné JL, Colin J, Laroche L, Montard M, Delbosc B, Aptel I, Ginisty H, Grandjean H, Malecaze F. Videokeratographic anomalies in familial keratoconus. Ophthalmology 2004; 111:867–874
90. Rabinowitz YS, Nesburn AB, McDonnell PJ. Videokeratography of the fellow eye in unilateral keratoconus. Ophthalmology 1993; 100:181–186
91. Rabinowitz YS, Garbus J, McDonnell PJ. Computer-assisted corneal topography in family members of keratoconus. Arch Ophthalmol 1990; 108:365–371
92. Uçakhan ÖÖ, Çetinkor V, Özkan M, Kanpolat A. Evaluation of Scheimpflug imaging parameters in subclinical keratoconus, keratoconus, and normal eyes. J Cataract Refract Surg 2011; 37:1116–1124
93. Kovács I, Miháltz K, Németh J, Nagy ZZ. Anterior chamber characteristics of keratoconus assessed by rotating Scheimpflug imaging. J Cataract Refract Surg 2010; 36:1101–1106
94. Koller T, Iseli HP, Donitzky C, Papadopoulos N, Seiler T. Topography-guided surface ablation for Forme Frustre Keratoconus. Ophthalmology 2006; 113:2198–2202
95. Randleman JB, Rusell B, Ward MA, Thompson KP, Stulting RD. Risk factors and prognosis for corneal ectasia after LASIK. Ophthalmology 2003; 110:267–275
96. Malecaze F, Coullet J, Calvas P, Fournié P, Arné JL, Brodaty C. Corneal ectasia after photorefractive keratectomy for low myopia. Ophthalmology 2006; 113:742–746
97. Bilgihan K, Özdek SC, Konuk O, Akata F, Hasanreisoglu B. Results of photorefractive keratectomy in keratoconus suspects at 4 years. J Refract Surg 2000; 16:438–443
98. Weed KH, McGhee CNJ, MacEwen CJ. Atypical unilateral superior keratoconus in young males. Cont Lens Anterior Eye 2005; 28:177–179
99. Prisant O, Legeais J-M, Renard G. Superior keratoconus. Cornea 1997; 16:693–694
100. Charles N, Charles M, Croxatto O, Charles DE, Wertheimer D. Surface and Orbscan II slit-scanning elevation topography in circumscribed posterior keratoconus. J Cataract Refract Surg 2005; 31:636–639
101. Butler TH. Keratoconus posticus. Trans Ophthalmol Soc U K 1930; 50:551–556
102. Mannis MJ, Lightman J, Plotnik RD. Corneal topography of posterior keratoconus. Cornea 1992; 11:351–354
103. Collins MJ, Buehren T, Trevor T, Statham M, Hansen J, Cavanagh DA. Factors influencing lid pressure on the cornea. Eye Contact Lens 2006; 32:168–173
104. Lebow KA, Grohe RM. Differentiating contact lens induced warpage from true keratoconus using corneal topography. CLAO J 1999; 25:114–122
105. de Paiva CS, Harris LD, Pflugfelder SC. Keratoconus-like topographic changes in keratoconjunctivitis sicca. Cornea 2003; 22:22–24

First author:
David P. Piñero, PhD

Oftalmar, Department of Ophthalmology, Medimar International Hospital, Alicante, Spain